



Active paper packaging material based on antimicrobial conjugated nano-polymer/amino acid as edible coating

Saber Ibrahim^a, Houssni El Saied^b, Mohamed Hasanin^{b,*}

^a Packaging Materials Department, National Research Centre, 12622, Dokki, Cairo, Egypt

^b Cellulose and Paper Department, National Research Centre, 12622, Dokki, Cairo, Egypt

ARTICLE INFO

Article history:

Received 14 July 2018

Accepted 15 October 2018

Available online 17 October 2018

Keywords:

Active packaging

Conjugated polymer/amino acid

Antimicrobial activity

And coating paper

ABSTRACT

Conjugated amino acid with nano-biodegradable polymer was applied as ecofriendly and edible coating. Polystyrene sulfate (PSS) was highly investigated with dynamic light scattering (DLS) to measure the particle size and over charge (zeta potential measurements) of nano-polymer system as well as the homogeneity of particle distribution in presence and absence of Lysine mixture (AA). In addition, topographical structure of the coating was studied for PSS, AA and conjugated one as well as Fourier transform infrared (FTIR) and Differential Scanning Calorimetry (DSC). Antimicrobial test cleared that the prepared conjugate described as broad-spectrum antibacterial agent as well as antifungal with different concentrations. The hydrophilic active ingredient is absorbed into fiber, distributed homogenously and kept out the fiber loaded with antimicrobial properties over all areas. Tensile strength of the paper sheets coated with unilayer 200 μ thickness presented good improving in physical and mechanical properties of coated paper sheets as well as gives more fiber condensation according to Scanning Electron Microscope (SEM) topography.

© 2018 The Authors. Production and hosting by Elsevier B.V. on behalf of King Saud University. This is an open access article under the CC BY-NC-ND license (<http://creativecommons.org/licenses/by-nc-nd/4.0/>).

1. Introduction

Packaging is the processing in which some technologies are used for enclosing or maintain the original product state luster till arrives to consumer (Choi and Burgess, 2007; Youssef and El-Sayed, 2018). Recyclable packaging material is new challenge where the reprocessing of materials (pre- and post-user) offer new products (Twede et al., 2014). Some materials such as steel, aluminum, papers, plastics, etc. are the largest primary components of a package, but the huge amounts of this components cannot be recycled because they are difficult to separate and do contaminate (Othman, 2014). Packages can sometimes be designed to separate components to better facilitate recycling. Additionally some of packaging materials are harmful to use as food contact otherwise it may be help the food to rot (Ibrahim et al., 2017,

2016). Free additives paper is the safest recycling packaging materials, which have not any hazard additives e.g. heavy metal, non-degradable petroleum polymers, and toxic materials as well as can be used as food contact. Nevertheless, the free additive papers have high safety profile as food contact but have many disadvantages in packaging such as, not resistant to microorganisms attacking and poisons as well as low mechanical and physical properties (Abou-Zeid et al., 2018; Youssef et al., 2019). Coating of paper with bio-base biological active coating may be reducing many disadvantages of free additive papers, since the traditional coating materials are mostly containing hazard and toxic materials (Abou-Zeid et al., 2018; Youssef et al., 2018; Youssef, Kamel, and El-Samahy, 2013). The convention antimicrobial coating in most preservation process is heavy metal ions and the drawback of this process is release of metal ions and contaminate throughout the food (Barhoum et al., 2014). In addition, to some paper surface coating is normally accompanied by some disadvantages such as, high porous structure, poor microbial resistance and low mechanical properties. These drawbacks negatively affect the quality of the paper used in food preservation mostly for food contact applications (El-Saied et al., 2003). Dual role coating materials e.g. bio-based composite has recently been employed for food packaging because it has various favorable properties such as biodegradability, renewability, recyclability, and mechanical flexibility as well as not

* Corresponding author at: Cellulose & Paper Dept., National Research Centre, El-Buhouth St., Dokki, 12622, Egypt.

E-mail address: sido_sci@yahoo.com (M. Hasanin).

Peer review under responsibility of King Saud University.



cytotoxic and safe as food contact materials (Abou-Zeid et al., 2018; Wacoo et al., 2014). Various strategies have recently begun to synthesis non-toxic with anti-microbial properties coating the paper sheet to enhance its properties for food preservation avoid the heavy metal ions hazardous (Gomez-Carretero et al., 2017; Khalid et al., 2016; Levдик et al., 1967). Biomaterials, such as amino acids have unique features emerged as sustainable. Biocompatible and biocompatible are the main characters which draw attention to these materials to use as alternatives to plain petroleum-based polymers in biomaterials (Ghorab et al., 2004; Rehimi et al., 2015). Amino acids are excellent example to these compounds (El-Henawy et al., 2018; Wu, 2009). Lysine is one of the essential amino acid which has not any toxically affect as well as having high biological important and also uses as nutrient supplant with great safety profile (Abelson, 1999). On the other hand, the most promising and interesting biodegradable as well as biocompatible polymers is sodium polystyrene sulfate which is sodium salt of polystyrene sulfate (PSS) derived from polystyrene by addition of sulfonate functional groups (Girard et al., 2013). PSS used as drug without any additive as well as approved from food and drug administration (FDA) as nutrient and drug (Sterns et al., 2010). PSS widely used as ion-exchange resins to remove ions such as potassium, calcium, and sodium from solutions in technical or medical applications (De Dardel and Arden, 2008). Bulky group growth inhibition technique is the new promising field in anti-biological activity applications (Basta et al., 2016; Nelson and O'Connor, 1964b; Van de Loosdrecht et al., 1994) without any toxic effect. Using of excellent edible and highly safety profile materials as biobased-bioactive paper coating is added important value in active packaging and edible paper coating. Conjugation between PSS and amino acid is discussed in the present work as new trend and the most important challenge for using biodegradable, biocompatible, food contact and not cytotoxic materials as coating paper sheets with improving the mechanical and physical properties to use as food contact and preserved coated paper.

2. Materials

Paper sheets are delivered from Quena Co. for paper production- Upper Egypt. Sodium salt of poly styrene sulfate (PSS) was purchased from AldrichCo., lysine mixture (AA) (monohydrochloride and base) purchased from BDH, Biochemical, England. All medium and its components were purchased from modern Lab Co, India.

2.1. Preparation of PSS lysine conjugate (Conj.)

PSS-AA Conjugate was prepared, using PSS and AA with different ratios (1: 1.25, 1.5, 1.75, 2.0, 2.5, and 3.0) PSS and Lysine respectively. Fusion method was carried out according to Basta et al., (Basta et al., 2016) by mixing PSS with different ratios AA, for 1.5 h at about 250 °C, then the product was subjected to microwave for about 30 s/g_{mixture}. The resulted conjugates were washed several times by Millipore water, and air dried. Antimicrobial test was carried out as described below to select the promising coater as lasted in (Table 1).

Minimal inhibition concentration (MIC) calculation was carried out via plat diffusion method, Gram-positive and Gram-negative bacteria as well as uni-cellular fungi are presented. Five microorganisms are tested against conjugate *Bacillus subtilis* (NCID-3610) and *Staphylococcus aureus* (NCTC-7447) as Gram positive and *Escherichia coli* (NCTC-10416) and *Pseudomonas aeruginosa* (NCID-9016) as Gram-negative bacteria as well as *Candida albicans* (NCCLS 11) were used as unicellular fungi. One colony of each microbial strain was suspended in a physiological saline

Table 1
Effect of PSS/amino acid ratio on microbial activity of PSS-Lysine conjugate.

Exp. No.	PSS	Lysine	A
1	1	1.25	UD ^a
2	1	1.5	UD
3	1	1.75	UD ^b
4	1	2.0	D
5	1	2.5	D
6	1	3	D

^a Antimicrobial activity undetected (absence of inhibition zone).

^b Antimicrobial activity detected (present zone detected).

solution (NaCl 0.9% in distilled water at pH 6.5). The initial tested concentration of the PSS-AA was 100ug/ml. The MICs were calculated as stated previously (Basta et al., 2016; Remmal et al., 1993). Different concentrations (100, 50, 25, 12.5, 6.25, 3.125, 1.5625, 0.78125, 0.390625, 0.195313, 0.097656, and 0 µg/ml as positive control) of the tested conjugate were prepared through serial dilution method. Mueller Hinton Agar medium was inoculated by the above-mentioned bacterial strains and fungi are incubated individually at 37 °C for 24 h. After all incubation periods have been elapsed clear zones were measured in mm. The above concentrations were used to determine the MIC value under the same incubation conditions.

2.2. Characterization of coating

Fourier transform infrared (FTIR): The structure change between PSS, AA and its conjugated polymer was studied by attenuated total reflectance Fourier transform infrared (ATR-FTIR) spectroscopy (Spectrum Two IR Spectrometer – PerkinElmer, Inc., Shelton, USA). All spectra were obtained by 32 scans and 4 cm⁻¹ resolution in wave numbers ranging from 4000 to 450 cm⁻¹. IR measurements which are including crystallinity index (Cr.I.) (Nelson and O'Connor, 1964a,b; Razva et al., 2014) and main hydrogen bond strength (MHBS) (Levdik et al., 1967) were calculated.

Differential Scanning Calorimetry (DSC): The DSC instrument (SETRAM DSC evo-131, France) with scan rate 5 °C/min was used to study the thermal behavior of PSS, AA and its conjugate compound/s.

Surface modification study (SEM): The morphology and topography of the prepared samples were analyzed by scanning electron microscopy (SEM, Quanta FEG 250, FEI). The SEM sample, a thin layer of Au was coated onto the sample by sputtering coating unit.

2.2.1. Particle size distribution and zeta potential measurements

The particle size distribution and zeta potential of the prepared samples were measured, using Nicomp™ 380 ZLS size analyzer, USA. Leaser light scattering was used at 170° in case of particle size detection where zeta potential was measured at 18°.

2.3. Paper coating

Coating formulation: PPS and AA was dissolved in aqueous medium (5 g in 100 ml) as separated solutions. Conjugated coating was prepared with solid content 5% (wt/wt) by mixing with water together under ultrasonic homogenizer Qsonics, USA (4 min/ 70% amplitude).

Coating process: Automatic film applicator (SMF-VII, 310) with different road coaters (150 and 200 µm) was used. Paper sheet was fixed over vacuum plate and applied constant speed in forward and backward movements. According to solid content calculation, coating thickness was varied as 150 µ and 200 µ coating thickness. The paper sheets were coated with one, two and three

coating layers. Coated paper sheets were dried in thermal drying in air circulation oven at 80 °C for complete drying to avoid paper deformation.

2.4. Coating sheets testing

The mechanical properties, including tensile strength, Young's modulus (using universal Instron testing machine), Roughness, and burst index as well as physical properties (water absorption and air permeability) were determined. Surface morphology of coated paper sheets were investigated with SEM as mentioned above. Morphological study of coating paper sheets was carried out as mentioned previously in SEM topography.

3. Results and discussion

3.1. Preparation of conjugate

Optimizing the PSS and AA suitable fusion ratio was judged with the response of tested microorganisms detected as listed in (Table 1). The conjugate was getting his anti-microbial activity from bulky group growth inhibition mode of action (Hyldgaard et al., 2014). The bulky group growth inhibition is new promising field in antibiological activity applications (Hyldgaard et al., 2014; Salama, 2017). This application depends on the formation of conjugate from two substances, one of important biological role (AA), while the other one (PSS) not only has bulky characters but also biocompatible. Each conjugate procure component has not any antimicrobial activity, Exp. 1, 2, and 3 were shows undetected microbial sensitivity. This could have happened as a result of high concentration of AA which consumed by microorganism as nutrient in Free state. Exp. 4 show the suitable ratio in which the conjugation giving antimicrobial activity with lowest amount of amino acid. It is form interested economical point of view. Moreover, the prepared conjugate has new physical, chemical, and biological characters which emphasized conjugate is prepared.

3.2. Coating characterization

3.2.1. Antimicrobial and MIC calculation

The antimicrobial activity of this prepared conjugate was tested against microbial strains with different concentrations. MIC was calculated with measuring the surrounded clear inhibition zone diameter which refers to conjugate activity against tested organism (s), as shows in (Table 2 and Fig. 1). The obtained data shows that novel conjugate has strongest inhibitory effect on broad spectrum bacteria (Gram positive and negative). Where the antimicrobial activity against gram positive with MIC 25 µg/ml for *Bacillus*

subtilis (NCID-3610) and 12.5 µg/ml for *Staphylococcus aureus* (NCTC-7447). These values are highly prospective values according to (Basta et al., 2018). While, for the case of gram negative bacteria the MIC value for *Escherichia coli* (NCTC-10416) was 50 µg/ml, as well as for *Pseudomonas aeruginosa* (NCID-9016) was 12.5 µg/ml and this was in agreement with (El-Saied et al., 2003; Rowlinson et al., 2003). Moreover, this conjugate showed significant activity against unicellular fungi *Candida albicans* (NCCLS 11), where its MIC was 3.125 µg/ml. The antimicrobial activity of the investigated conjugate ascribed to the presence of bulkier PSS molecules, which interprets the metabolic pathway and makes cells lost their ability to progress over stopping the protein building up using the bulky group (PSS) to block the active side of amino acid binding site (Hyldgaard et al., 2014; Menninger, 1995). Thereby, resulting significant activity is appeared. This explanation is in agreement with that reported for the role of bulky group and the exact relationship between bulk structure of agent and its inhibition activity as well as the conjugate can be described as broad-spectrum antimicrobial agent.

3.2.2. FTIR

The FT-IR spectra were illustrated in (Fig. 2), spectrum of PS-SO₃H powders were taken over the range of wavenumbers from 450 to 4000 cm⁻¹, but for the analysis of sulfonic groups, spectrum was shown over the range from 800 and 1400 cm⁻¹. Sulfonic group vibration bands are reported at approximately 1040 and 1180 cm⁻¹ (Martins et al., 2003). The characteristic infrared absorbance for PS-SO₃H have suggested the bonding of the sulfonic groups to the aromatic ring of PS (out of plane deformation bands assigned to substituted aromatic ring γ (C-H) at wavenumbers approximately from 830 to 850 cm⁻¹). The absorption at 1040 cm⁻¹ resulted from the symmetric stretching vibration of SO₃H groups and the absorption at 1127 cm⁻¹ results from a sulfonate anion attached to a phenyl ring. Our results are in agreement with the literature ones (Pantelić et al., 2009). We verified that the ν_{as}(S–O) vibration at 1180 cm⁻¹ appears as a very broad band at approximately 1100 cm⁻¹–1350 cm⁻¹. AA shows the traditional amino acid IR spectra, however shows bands at 3316, 2944, 2104, 1576, and 1516 cm⁻¹ which refer to (O and N)–H, CH₂, C–H symmetrical deformation, and C=O respectively as well as fingerprint bands (Kitadai et al., 2009; Mostafa et al., 2017a,b). Consequence of after conjugation process, some function groups and new bands are appeared, as well as some are vanished. Conjugate spectra show bands positions as well as band sharpness were different than two started materials. Conjugate showed some changes in bands in the rang 4000–3000 cm⁻¹ which regarded to OH stretching vibration, NH vibration in AA and C–H in PSS, this is in agreement with IR calculations (MHBS and Cr.I.) in (Table 3) which

Table 2

MIC (µg/ml) of conjugated compound on tested bacteria and fungi, inhibition zone diameters were recorded in (mm).

MIC µg/ml	inhibition zone/mm				
	<i>B. subtilis</i> NCID-3610	<i>S. aureus</i> NCTC-7447	<i>P. aeruginosa</i> NCID-9016	<i>E. coli</i> NCTC-10416	<i>C. albicans</i> NCCLS 11
100	12 ± 0.9	19 ± 1.66	19 ± 1.1	17 ± 0.8	31 ± 2.3
50	9 ± 1.0	11 ± 1.1	11 ± 0.7	10 ± 0.6	22 ± 1.4
25	5 ± 0.4	7 ± 0.92	5 ± 0.39	0	17 ± 0.8
12.5	0	4 ± 0.55	3 ± 0.3	0	9 ± 1.11
6.25	0	0	0	0	6 ± 0.99
3.125	0	0	0	0	4 ± 0.7
1.5625	0	0	0	0	0
0.78125	0	0	0	0	0
0.390625	0	0	0	0	0
0.195313	0	0	0	0	0
0.097656	0	0	0	0	0
0	0	0	0	0	0

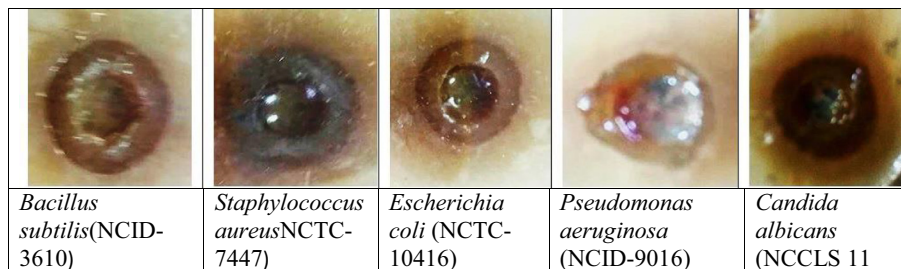


Fig. 1. MIC antimicrobial test for conjugate (well diffusion method).

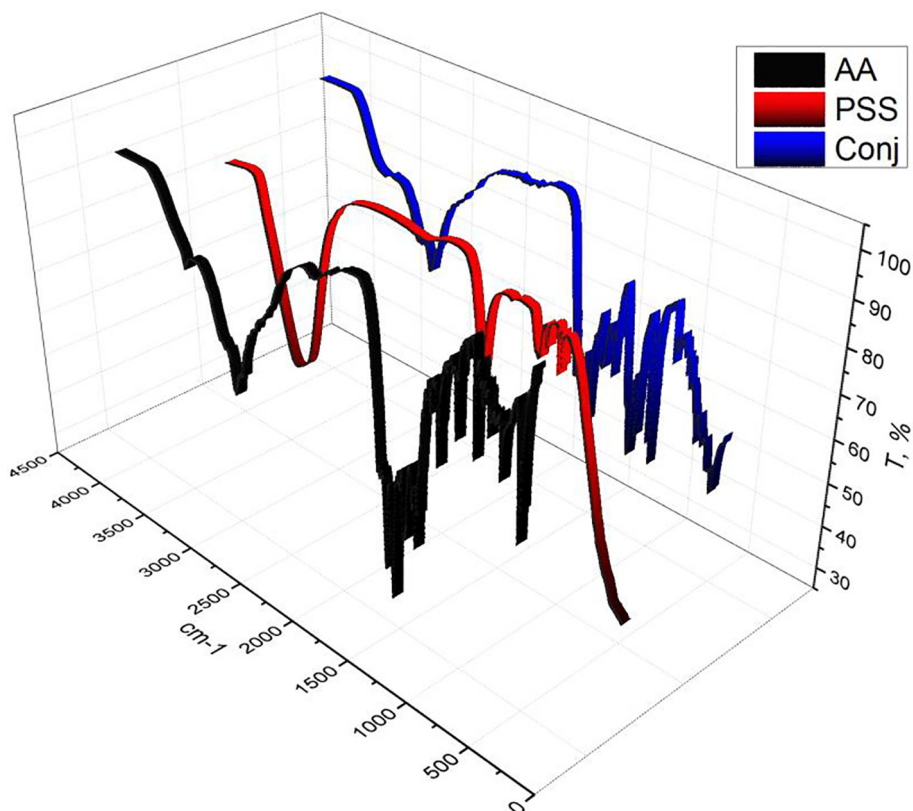


Fig. 2. FTIR spectra for Amino acid, PSS, and conjugated compound.

Table 3
FTIR calculation of PSS, Amino acid and conjugated coating.

Sample	crystal index	MHBS
PSS	0.91	5.44
Lysine	0.79	3.06
Conjugate	1.67	4.49

are increased in conjugate in result of OH starching vibration and NH vibrations, this is emphasized that the increased of MHBS value of conjugate which increased than AA and decreased than PSS. Cr.I. value of conjugate was duplicated, this results is in agreement with SEM image. Blue shift is appeared in conjugate band at 3457 cm^{-1} which observed in PSS and AA at 3307 and 3358 cm^{-1} respectively. This may lead to liberate the hydrogen bonds during synthesis process. The bands which are characterized to sulfonate group in PSS show some changes in follow bands; 1192 , 1124 , 1034 , and 1009 which have become sharper and recorded insanity higher than PSS spectra, this may be related to formation of crystal as mentioned. The forgoing data illustrated that the reaction between

PSS and AA was going out via $-\text{SO}_3\text{Na}$ in PSS and $-\text{COOH}$ group in AA and produces NaOH. Other evident is the pH of solution of conjugated material before washing was more than 8 whilst the pH of AA and PSS before reaction was less than 6.5 (Dhawan, 2002).

3.2.3. DSC

(Fig. 3) showed the three DSC curves for started materials and conjugate. PSS curve shows after adsorbed water region only one peak with onset $136.25\text{ }^\circ\text{C}$ and offset $180.7\text{ }^\circ\text{C}$ with as well as peak temperature (T_p) $158.5\text{ }^\circ\text{C}$. Similarly, in AA the DSC curve has one hump peak with T_p $105.76\text{ }^\circ\text{C}$. Additionally, conjugate curves show completely difference from both started materials. Clear splitting of started materials main peak to two peaks was appearing in conjugate DSC curve this accentual the produce new conjugate (Hatakeyama and Hatakeyama, 1990). Moreover, no significant variation in onset and outset values as shown in (Table 4). However, heat capacity is recorded with high value 117.46 J/g in conjugate one, comparison with started materials PSS and AA are 14.99 and 4.909 J/g respectively. This emphasized that the reaction

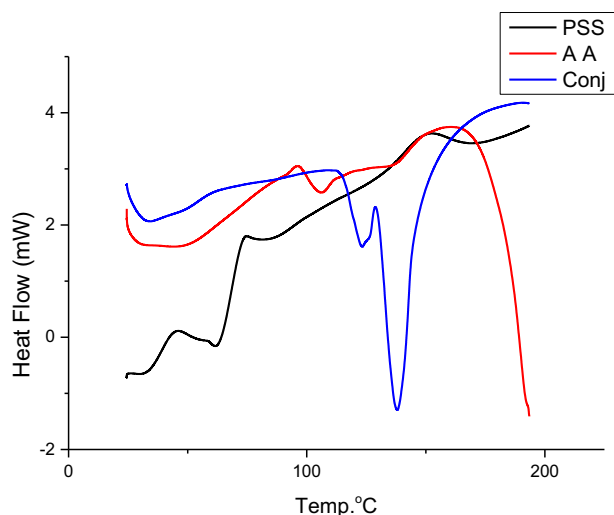


Fig. 3. DSC curves for started materials and conjugate.

between PSS and AA give highly thermal stable conjugate with high activation energy value as stated before (Garg et al., 2005).

3.2.4. DLS and zeta potential

DLS results were plotted in (Fig. 4), polydispersity index (PDI) and mean particle size were lasted in (Table 5). The PDI is a measure of dispersion homogeneity. PDI value is ranged from 0 to 1.0 where from 0 to 0.3 is refer to the highest homogeneity distribution state (Cheng et al., 2018). The narrow uniform Gaussian distribution can be pointed to low PDI especially for PSS, and AA. as shown in (Fig. 3). Additionally, conjugated coating still presents few particle size variations with little higher PDI in related to AA and PSS as lasted in (Table 5). The mean diameters were measured in aqueous solutions with relative concentration as 439, 340 and 527 nm for PSS, AA and conjugated coating particles, respectively. Additionally, zeta potential was calculated from the three main

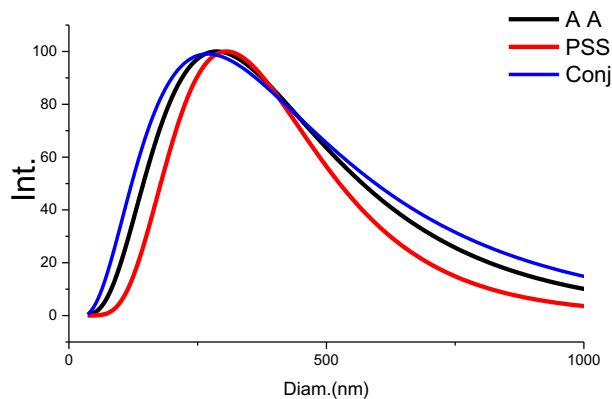


Fig. 4. DLS for Amino acid, PSS, and conjugated compound.

Table 4

DSC measurements of PSS, amino acid and conjugated coating.

Code	T_g (°C)	T_i (°C)	T_p (°C)	ΔT (°C)	Heat capacity (J/g)
Lysine	98.11	112.19	105.76	14.08	4.909
PSS	136.25	180.74	158.5	44.49	14.99
Conjugate	128.98	145.98	137.77	17.0	117.46

measured factors (cell current, phase shift and mobility) that depending on the charge over particles. Zeta measurements of PSS, AA and conjugated coating were tabulated in (Table 5) and all related factors. Sulfonated group play a vital role in the net charge of PSS to be -0.68 mV where AA presented average zeta potential -12.48 mV. Combined system was detected at -7.38 mV which pointed to the connection side from COO^- that reduced the value from -12 to -7.38 mV. FTIR supported this assumption by little decrease in $\text{C}=\text{O}$ bond in conjugated chart than AA peak.

3.2.5. Microstructure investigation

PSS polymer showed nano-polymer in scale around 25 nm however after conjugation interaction between protein and polymer give uniform aggregated particles with as shown in (Fig. 5). Conjugated coating paper uniform particle in micron rang size with core/shell form as shown in (Fig. 5-E and F). Core size was recorded 689 nm while shell diameter was 3675 nm which confirmed in result to drying sample and aggregates the particles as core/shell form and distribute in solutions as colloids. These results have nice agreements with particle size distribution over DLS for AA and conjugate. However the results of PSS which show in (Fig. 5-A and B) in opposed to the DLS data this may be takes place as result of highly surface area either aggregate phenomena of PSS in water (Sen et al., 2007) as well as water hydrophilic properties of PSS which performed to swelling and recorded particle size more than SEM topography.

3.3. Coated paper evaluation

3.3.1. Coating sheets properties

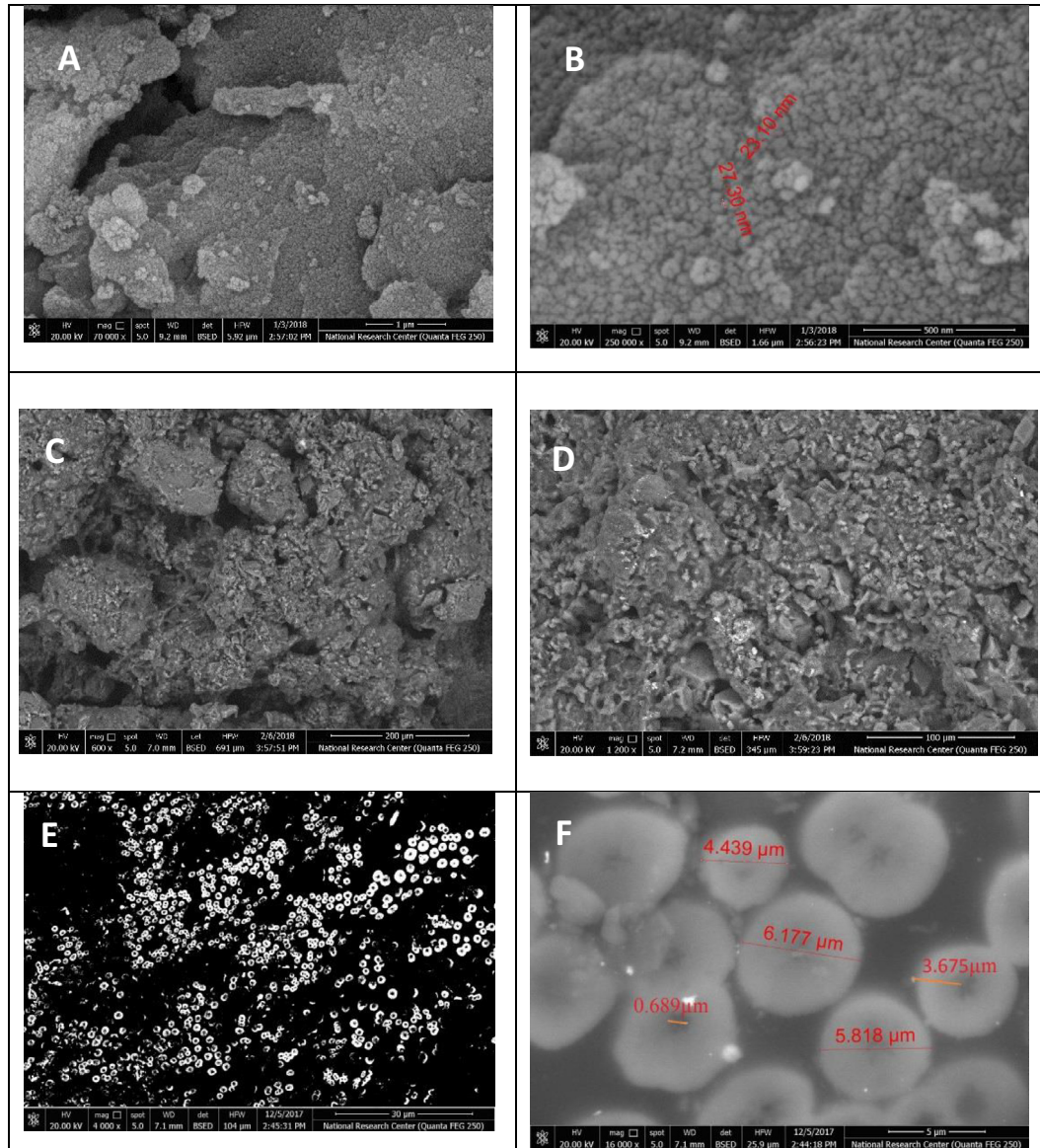
The mechanical properties, including tensile strength, Young's modulus, roughness, and burst index were carried out for uncoated (blank) and coating papers sheets. The results were calculated and displayed in (Table 6). Tensile strength of the paper sheets coated with 1 layer 150 and 200 μm thickness was increased by about 2% and 17%, respectively in comparing to the blank paper sheets. Additionally, the Young's modulus was also increased by about 19% and 22%, respectively. On the contrary were the both thickness (150 and 200 μm) of two and three layers sheets drawback are noticed in the tensile strength and Young's modulus. This is referring to the high swelling degree of paper fiber in two and three coating layers on papers sheets. This is due to water base coating conjugate which penetrates the fibers easily. Moreover, the hydrophilic coating gives the paper fiber highly microbial resistance. Where the active ingredient is adsorbed into fiber and distributed homogenously and kept out the fiber loaded with antimicrobial properties over all fibers areas. In one-layer paper sheets, paper fibers shape converted from flat form to round form, which help in compact the fibers together and became closed than in blank sheets. Antithesis in the two and three layers coated paper sheets, increasing in coating layers give significant draw back variations because paper fibers have over swell with coating matrix and become fragile.

On the other hand increasing the coating thicknesses gives significant variation in roughness values in comparison with reference sheets value (Abou-Zeid et al., 2018; Barhoum et al., 2014). One layer paper sheets roughness of 200 μm coating thickness increased with 13 times than 150 μm thickness. Additionally, double layers paper sheets with coating thickness 200 μm show increase in roughness value with 8 times than 150 μm thickness ones. Triple layers paper sheets showed less improvement with 4 times only. Burst index shows monotonous values, this may be takes place according to the swelling of fibers in all layers types lead to close all pours. However water absorption gives high values for coated paper sheets than blank one, the reason of this phenom-

Table 5

Shows zeta potential measurements of PSS, amino acid and conjugated coating.

	zeta potential measurements				Particle size measurements	
	Cell current, mA	Av. Phase shift, rad/sec	Av. Mobility, M.U.	Av. Zeta potential, mV	PDI	Average particle size/nm
Lysine	8.95	-2.39	-0.05	-0.68	0.21	439
PSS	9.67	-23.11	-0.87	-12.48	0.34	340
Conjugate	17.13	-22.67	-0.52	-7.38	0.46	527

**Fig. 5.** SEM for PSS at low magnification (A), high magnification (B), amino acid at low magnification (C), high magnification (D), and Conjugate at low magnification (E), High magnification (F).**Table 6**

Mechanical and physical properties of uncoated paper and coated paper.

	Tensile strength (MPa)	Young's modulus (MPa)	Roughness	Burst index (KPa.m ² /g)	Water absorption (g/m ²)	Air permeability (ml/min)
Reference Paper	23.15 ± 1.92	2.05 ± 0.77	10	312	21	94 ± 2.44
PSS	25.17 ± 1.7	2.78 ± 0.92	41	308	36	87 ± 2.21
1 Layer 150 μ	23.44 ± 1.81	2.49 ± 0.44	31	Less than 200	40	53.5 ± 2.51
1 Layer 200 μ	27.12 ± 2.19	2.43 ± 0.49	412	Less than 200	55	27.5 ± 2.12
2 Layer 150 μ	20.85 ± 0.97	1.81 ± 0.19	51	Less than 200	45	32.5 ± 0.77
2 Layer 200 μ	12.81 ± 2.11	1.61 ± 0.14	412	Less than 200	60	30.5 ± 2.71
3 Layer 150 μ	9.3 ± 2.13	1.35 ± 0.21	108	Less than 200	50	46 ± 2.43
3 Layer 200 μ	10.38 ± 1.21	1.31 ± 0.23	434	Less than 200	59	60.5 ± 2.12

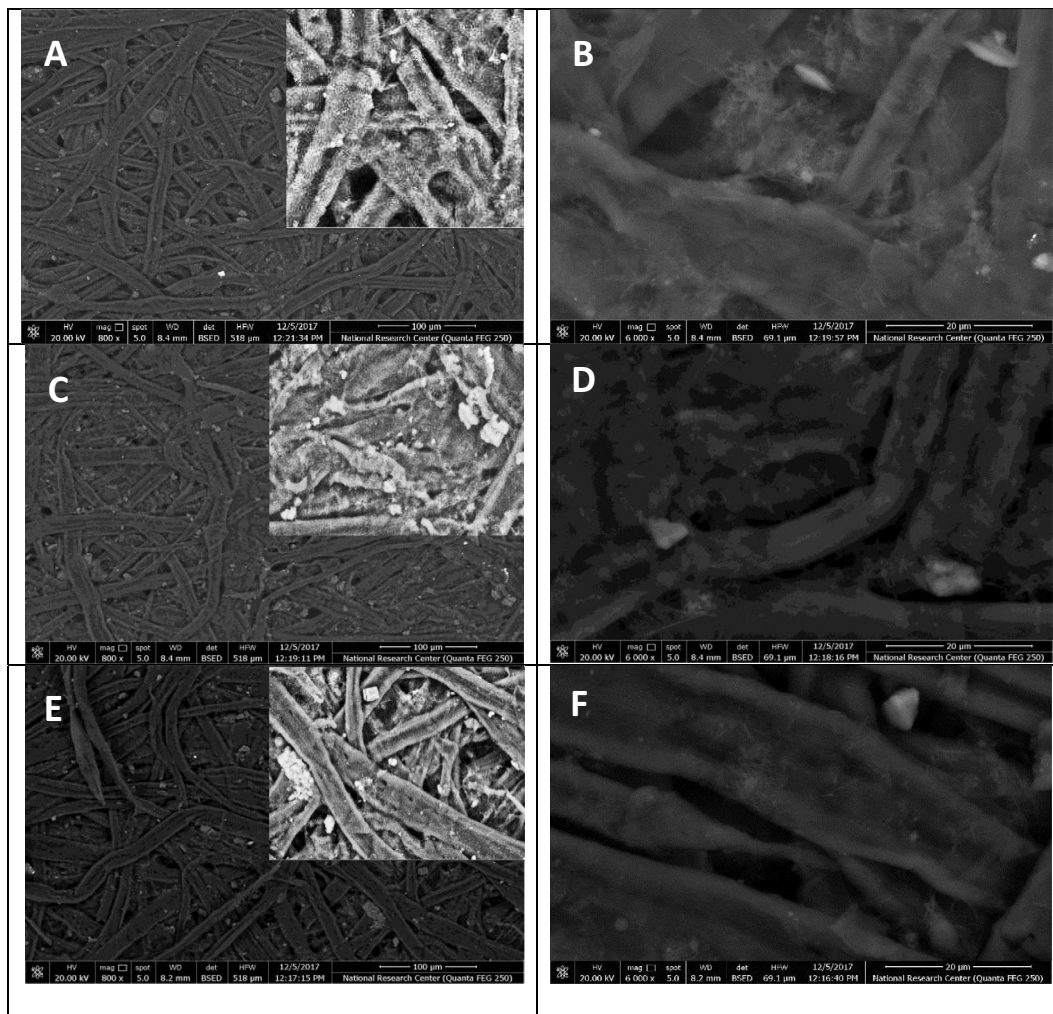


Fig. 6. SEM for blank paper sheet at low magnification (A), high magnification (B), 1 layer with 150 μ thickness at low magnification (C), high magnification (D), and 3 layers with 200 μ thickness. at low magnification (E), high magnification (F).

ena is similar to what happened in mechanical properties layers behaviors (Khwaldia Bet al., 2014). In addition, coating thickness and water absorption are directly proportion together. Air permeability in one layer paper sheets with coating thickness 200 μ m was the lowest value, this is an advantage can synergized the antimicrobial properties of paper coated sheets (Basta et al., 2015; El-Gendy et al., 2017) as well as reinforce preservation characteristics behavior.

3.3.2. Coating sheets morphology

SEM image (Fig. 6) displays surfaces morphological structure of blank paper sheet (Fig. 6-A and B) and papers coated with one layer with 200 μ m thickness (Fig. 6-C and D) and three-layer 150 μ thickness (Fig. 6-E and F) conjugate. Blank shows a typical morphology of the normal papers, which is a flat fiber network with free pores (Abou-Zeid et al., 2018). The fibers of coated papers were presented with thick diameter, that is can be attributed to highly soluble of conjugate which obtained from PSS (Essafi et al., 2009).

Conjugate can be penetrating paper fibers and filling space of paper filament after drying. This is elucidating the roughness values as well as air permeability results. SEM images were emphasized the mechanical and physical measurements. In addition, this phenomenon enhanced the antimicrobial efficiency not only as a coating but also at active filler between cellulose fibers.

4. Conclusion

Active coating of papers sheets with prepared conjugate is promising technique for producing safety antimicrobial and biocompatible packaging materials suitable to be used as food contact. The treated papers sheets are characterized by improved physical and mechanical properties as well as microbial resistance and antimicrobial behavior.

Acknowledgment

The authors express their sincere thanks to National Research Centre Of Egypt for providing the necessary research facilities. The authors would like to acknowledge the facilities available at Central Laboratory Network (CLN), National Research Centre, Dokki, Giza, Egypt.

References

- Abelson, P.H., 1999. A potential phosphate crisis. *Science* 283 (5410), 2015.
- Abou-Zeid, R.E., Diab, M.A., Mohamed, S.A., Salama, A., Aljohani, H.A., Shoueir, K.R., 2018. Surfactant-assisted poly (lactic acid)/cellulose nanocrystal bionanocomposite for potential application in paper coating. *J. Renewable Mater.*
- Barhoum, A., Rahier, H., Abou-Zaid, R.E., Rehan, M., Dufour, T., Hill, G., Dufresne, A., 2014. Effect of cationic and anionic surfactants on the application of calcium

- carbonate nanoparticles in paper coating. *ACS Appl. Mater. Interfaces* 6 (4), 2734–2744.
- Basta, A.H., Khwaldia, K., Aloui, H., El-Saied, H., 2015. Enhancing the performance of carboxymethyl cellulose by chitosan in producing barrier coated paper sheets. *Nord. Pulp Pap. Res. J.* 30 (4), 617–625.
- Basta, A.H., El-Saied, H., El-Defdar, M.M., El-Henawy, A.A., El-Sheikh, H.H., Abdel-Shakour, E.H., Hasanin, M.S., 2016. Properties of modified carboxymethyl cellulose and its use as bioactive compound. *Carbohydr. Polym.* 153, 641–651.
- Basta, A.H., El-Saied, H., Hasanin, M.S., El-Defdar, M.M., 2018. Green carboxymethyl cellulose-silver complex versus cellulose origins in biological activity applications. *Int. J. Biol. Macromol.* 107, 1364–1372.
- Cheng, S., Zhao, Y., Wu, Y., 2018. Surfactant-free hybrid latexes from enzymatically hydrolyzed starch and poly(butyl acrylate-methyl methacrylate) for paper coating. *Prog. Org. Coat.* 118, 40–47.
- Choi, S.J., Burgess, G., 2007. Practical mathematical model to predict the performance of insulating packages. *Packag. Technol. Sci.* 20 (6), 369–380.
- De Dardel, F., Arden, T.V., 2008. Ion exchangers. In: *Ullmann's encyclopedia of industrial chemistry*.
- Dhawan, S., 2002. Design and construction of novel molecular conjugates for signal amplification (II): use of multivalent polystyrene microparticles and lysine peptide chains to generate immunoglobulin-horse radish peroxidase conjugates. *Peptides* 23 (12), 2099–2110.
- El-Gendy, A., Abou-Zeid, R.E., Salama, A., Diab, M.A.-H.A.-R., El-Sakhawy, M., 2017. TEMPO-oxidized cellulose nanofibers/poly(lactic acid)/TiO₂ as antibacterial bionanocomposite for active packaging. *Egypt. J. Chem.* 60 (6), 1007–1014.
- El-Henawy, A.A., Basta, A.H., El-Saied, H., Abdel-Shakour, E.H., Hasanin, M.S., El-Sheikh, H.H., 2018. Discovery potent of bagasse (CMC-L-Phe) as bioactive material based on DFT calculations. *Eurasian J. Anal. Chem.* 13 (5).
- El-Saied, H., Basta, A.H., Barsoum, B.N., Elberry, M.M., 2003. Cellulose membranes for reverse osmosis Part I. RO cellulose acetate membranes including a composite with polypropylene. *Desalination* 159 (2), 171–181.
- El-Saied, H., Mostafa, A.M., Hasanin, M.S., Mwafy, E.A., Mohammed, A.A., 2018. Synthesis of antimicrobial cellulosic derivative and its catalytic activity. *J. King Saud Univ. – Sci.*
- Essafi, W., Spiteri, M.-N., Williams, C., Boué, F., 2009. Hydrophobic polyelectrolytes in better polar solvent. Structure and chain conformation as seen by SAXS and SANS. *Macromolecules* 42 (24), 9568–9580.
- Garg, S., Vermani, K., Garg, A., Anderson, R.A., Rencher, W.B., Zaneveld, L.J.D., 2005. Development and characterization of bioadhesive vaginal films of sodium polystyrene sulfonate (PSS), a novel contraceptive antimicrobial agent. *Pharm. Res.* 22 (4), 584–595.
- Ghorab, M.M., Ismail, Z.H., Abdel-Gawad, S.M., Aziem, A.A., 2004. Antimicrobial activity of amino acid, imidazole, and sulfonamide derivatives of pyrazolo[3,4-d]pyrimidine. *Heteroat. Chem.* 15 (1), 57–62.
- Girard, J., Brunetto, P.S., Braissant, O., Rajacic, Z., Khanna, N., Landmann, R., Fromm, K.M., 2013. Development of a polystyrene sulfonate/silver nanocomposite with self-healing properties for biomaterial applications. *C. R. Chim.* 16 (6), 550–556.
- Gomez-Carretero, S., Nybom, R., Richter-Dahlfors, A., 2017. Electroenhanced antimicrobial coating based on conjugated polymers with covalently coupled silver nanoparticles prevents staphylococcus aureus biofilm formation. *Adv. Healthcare Mater.* 6 (20).
- Hatakeyama, T., Hatakeyama, H., 1990. Thermal and nuclear magnetic relaxation studies of water-sodium polystyrene sulfonate systems. *Polym. Adv. Technol.* 1 (5–6), 305–310.
- Hylgaard, M., Mygind, T., Vad, B.S., Stenvang, M., Otzen, D.E., Meyer, R.L., 2014. The antimicrobial mechanism of action of epsilon-poly-L-lysine. *Appl. Environ. Microbiol.* 80 (24), 7758–7770.
- Ibrahim, S., Sultan, M., Adeeb, Z., 2016. Water soluble cationic xylan-alginate polymer as packaging retardant-release peptide drug delivery. *Int. J. PharmTech Res.* 9 (5), 119–128.
- Ibrahim, S., Labeeb, A., Mabied, A.F., Soliman, O., Ward, A., Abd-El-Messieh, S.L., Abdelhakim, A.A., 2017. Synthesis of super-hydrophobic polymer nanocomposites as a smart self-cleaning coating films. *Polym. Compos.* 38, E147–E156.
- Khalid, H., Shamaila, S., Zafar, N., Sharif, R., Nazir, J., Rafique, M., Saba, H., 2016. Antibacterial behavior of laser-ablated copper nanoparticles. *Acta Metall. Sin. (English Letters)* 29 (8), 748–754.
- Khwaldia, K., Basta, A.H., Aloui, H., El-Saied, H., 2014. Chitosan-caseinate bilayer coatings for paper packaging materials. *Carbohydr. Polym.* 99, 508–516.
- Kitadai, N., Yokoyama, T., Nakashima, S., 2009. ATR-IR spectroscopic study of L-lysine adsorption on amorphous silica. *J. Colloid Interface Sci.* 329 (1), 31–37.
- Levdik, I., Inshakov, M., Misyurova, E., Nikitin, V., 1967. Study of pulp structure by infrared spectroscopy. *Tr. Vses Nauch. Issled. Inst. Tselyul. Bum. Prom* 52, 109–111.
- Martins, C.R., Ruggeri, G., De Paoli, M.-A., 2003. Synthesis in pilot plant scale and physical properties of sulfonated polystyrene. *J. Braz. Chem. Soc.* 14 (5), 797–802.
- Menninger, J.R., 1995. Mechanism of inhibition of protein synthesis by macrolide and lincosamide antibiotics. *J. Basic Clin. Physiol. Pharmacol.* 6 (3–4), 229–250.
- Mostafa, A.M., Yousef, S.A., Eisa, W.H., Ewaida, M.A., Al-Ashkar, E.A., 2017b. Synthesis of cadmium oxide nanoparticles by pulsed laser ablation in liquid environment. *Optik-Int. J. Light Electron Opt.* 144, 679–684.
- Mostafa, A.M., Yousef, S.A., Eisa, W.H., Ewaida, M.A., Al-Ashkar, E.A., 2017a. Au@CdO core/shell nanoparticles synthesized by pulsed laser ablation in Au precursor solution. *Appl. Phys. A* 123 (12), 774.
- Nelson, M.L., O'Connor, R.T., 1964b. Relation of certain infrared bands to cellulose crystallinity and crystal latticed type. Part I. Spectra of lattice types I, II, III and of amorphous cellulose. *J. Appl. Polym. Sci.* 8 (3), 1311–1324.
- Nelson, M.L., O'Connor, R.T., 1964a. Relation of certain infrared bands to cellulose crystallinity and crystal lattice type. Part II. A new infrared ratio for estimation of crystallinity in celluloses I and II. *J. Appl. Polym. Sci.* 8 (3), 1325–1341.
- Othman, S.H., 2014. Bio-nanocomposite materials for food packaging applications: types of biopolymer and nano-sized filler. *Agric. Agric. Sci. Procedia* 2, 296–303.
- Pantelić, N.A., Andria, S.E., Heineman, W.R., Seliskar, C.J., 2009. Characterization of Partially Sulfonated Polystyrene-block-poly (ethylene-ran-butylene)-block-polystyrene Thin Films for Spectroelectrochemical Sensing. *Anal. Chem.* 81 (16), 6756–6764.
- Razva, O., Anufrienkova, A., Korovkin, M., Ananieva, L., Abramova, R., 2014. Calculation of quartzite crystallinity index by infrared absorption spectrum. *IOP Conference Series: Earth and Environmental Science*. IOP Publishing, p. 012006.
- Rehim, M.H.A., Yousef, A.M., Ghanem, A., 2015. Polystyrene/hydrophobic TiO₂ 2 nanobelts as a novel packaging material. *Polym. Bull.* 72 (9), 2353–2362.
- Remmal, A., Bouchikhi, T., Rhayour, K., Ettayebi, M., Tantaoui-Elaraki, A., 1993. Improved method for the determination of antimicrobial activity of essential oils in agar medium. *J. Essent. Oil Res.* 5 (2), 179–184.
- Rowlinson, S.W., Kiefer, J.R., Prusakiewicz, J.J., Pawlitz, J.L., Kozak, K.R., Kalgutkar, A.S., Marnett, L.J., 2003. A novel mechanism of cyclooxygenase-2 inhibition involving interactions with Ser-530 and Tyr-385. *J. Biol. Chem.* 278 (46), 45763–45769.
- Salama, A., 2017. Dicarboxylic cellulose decorated with silver nanoparticles as sustainable antibacterial nanocomposite material. *Environ. Nanotechnol. Monit. Manage.* 8, 228–232.
- Sen, A.K., Roy, S., Juvekar, V.A., 2007. Effect of structure on solution and interfacial properties of sodium polystyrene sulfonate (NaPSS). *Polym. Int.* 56 (2), 167–174.
- Sterns, R.H., Rojas, M., Bernstein, P., Chennupati, S., 2010. Ion-exchange resins for the treatment of hyperkalemia: are they safe and effective? *J. Am. Soc. Nephrol.* 21 (5), 733–735.
- Twede, D., Selke, S.E., Kamdem, D.-P., Shires, D., 2014. *Cartons, Crates and Corrugated Board: Handbook of Paper and Wood Packaging Technology*. DESTech Publications Inc.
- Van de Loosdrecht, A., Beelen, R., Ossenkoppele, G., Broekhoven, M., Langenhuijsen, M., 1994. A tetrazolium-based colorimetric MIT assay to quantitate human monocyte mediated cytotoxicity against leukemic cells from cell lines and patients with acute myeloid leukemia. *J. Immunol. Methods* 174 (1–2), 311–320.
- Wacoo, A.P., Wendiro, D., Vuzi, P.C., Hawumba, J.F., 2014. Methods for detection of aflatoxins in agricultural food crops. *J. Appl. Chem.* 2014, 1–15.
- Wu, G., 2009. Amino acids: metabolism, functions, and nutrition. *Amino Acids* 37 (1), 1–17.
- Youssef, A.M., El-Sayed, S.M., 2018. Bionanocomposites materials for food packaging applications: concepts and future outlook. *Carbohydr. Polym.*
- Youssef, A.M., Kamel, S., El-Samahy, M.A., 2013. Morphological and antibacterial properties of modified paper by PS nanocomposites for packaging applications. *Carbohydr. Polym.* 98 (1), 1166–1172.
- Youssef, A.M., El-Sayed, S.M., El-Sayed, H.S., Salama, H.H., Assem, F.M., El-Salam, M. H.A., 2018. Novel bionanocomposite materials used for packaging skimmed milk acid coagulated cheese (Karish). *Int. J. Biol. Macromol.* 115, 1002–1011.
- Youssef, A.M., Assem, F.M., Abdel-Aziz, M.E., Elaaser, M., Ibrahim, O.A., Mahmoud, M., Abd El-Salam, M.H., 2019. Development of bionanocomposite materials and its use in coating of Ras cheese. *Food Chem.* 270, 467–475.